Delay effects in the response of low-grade gliomas to radiotherapy: a mathematical model and its therapeutical implications

Víctor M. Pérez-García*

Departamento de Matemáticas, Universidad de Castilla-La Mancha, ETSI Industriales, Avda. Camilo José Cela 3, 13071 Ciudad Real, Spain
*Corresponding author. Email: victor.perezgarcia@uclm.es

Magdalena Bogdanska

Mathematics Department, Technical University of Lodz, Lodz, Wolczanska 214 Street, Lodz, Poland

Alicia Martínez-González, Juan Belmonte-Beitia

Departamento de Matemáticas, Universidad de Castilla-La Mancha, ETSI Industriales, Avda. Camilo José Cela 3, 13071 Ciudad Real, Spain

Philippe Schucht

Universitätsklinik für Neurochirurgie, Bern University Hospital, CH-3010 Bern, Switzerland

AND

Luis A. Pérez-Romasanta

Radiotherapy Unit, University Hospital of Salamanca, Salamanca, Spain

Low-grade gliomas (LGGs) are a group of primary brain tumours usually encountered in young patient populations. These tumours represent a difficult challenge because many patients survive a decade or more and may be at a higher risk for treatment-related complications. Specifically, radiation therapy is known to have a relevant effect on survival but in many cases it can be deferred to avoid side effects while maintaining its beneficial effect. However, a subset of LGGs manifests more aggressive clinical behaviour and requires earlier intervention. Moreover, the effectiveness of radiotherapy depends on the tumour characteristics. Recently Pallud *et al.* (2012. *Neuro-Oncology*, **14**, 1–10) studied patients with LGGs treated with radiation therapy as a first-line therapy and obtained the counterintuitive result that tumours with a fast response to the therapy had a worse prognosis than those responding late. In this paper, we construct a mathematical model describing the basic facts of glioma progression and response to radiotherapy. The model provides also an explanation to the observations of Pallud *et al.* Using the model, we propose radiation fractionation schemes that might be therapeutically useful by helping to evaluate tumour malignancy while at the same time reducing the toxicity associated to the treatment.

Keywords: low-grade gliomas; radiotherapy; mathematical model of tumour response.

1. Introduction

Low-grade glioma (LGG) is a term used to describe WHO grade II primary brain tumours of astrocytic and/or oligodendroglial origin. These tumours are highly infiltrative and generally incurable but have a median survival time (ST) of >5 years because of low proliferation (Pignatti *et al.*, 2002; Pouratian

& Schiff, 2010). While most patients remain clinically asymptomatic besides seizures, tumour transformation to aggressive high-grade glioma is eventually seen in most patients.

Management of LGG has historically been controversial because these patients are typically young, with few, if any, neurological symptoms. Historically, a wait and see approach was often favoured in most cases of LGG due to the lack of symptoms in these mostly young and otherwise healthy adults. The support for this practice came from several retrospective studies showing no difference in outcome (survival, quality of life) if therapy was deferred (Olson *et al.*, 2000; Grier & Batchelor, 2006). Other investigations have suggested a prolonged survival through surgery (Smith *et al.*, 2008). In this absence of a randomized controlled trial, recently published studies may provide the most convincing evidence in support of an early surgery strategy (Jakola *et al.*, 2012) and waiting for the use of other therapeutical options such as radiotherapy and chemotherapy. However, the decision on the individual treatment strategy is based on a number of factors including patient preference, age, performance status and location of tumour (Ruiz & Lesser, 2009; Pouratian & Schiff, 2010).

As to radiation therapy the clinical trial by Garcia *et al.* (2004) showed the advantage of using radiotherapy in addition to surgery. However, the timing of radiotherapy after biopsy or debulking is debated. It is now well known that immediate radiotherapy after surgery increases the time of response (progression-free survival), but does not seem to improve overall survival while at the same time inducing serious neurological deficits as a result of normal brain damage (Van den Bent, 2005). Overall survival depends more on patient- and tumour-related characteristics such as age, tumour grade, histology and neurological function than the details of the plan of radiotherapy treatment. Radiotherapy is usually offered for patients with a combination of poor risk factors such as age, sub-total resection and diffuse astrocytoma pathology (Higuchi *et al.*, 2004).

Mathematical modelling has the potential to select patients who may benefit from early radiotherapy. Also it may help in developing specific optimal fractionation schemes for selected patient subgroups. However, despite its enormous potential, mathematical modelling has had a limited use with strong focus on some aspects of radiation therapy (RT) for high-grade gliomas (Barazzuol *et al.*, 2010; Konukoglu *et al.*, 2010; Rockne *et al.*, 2010; Bondiau *et al.*, 2011). Up to now, no ideas coming from mathematical modelling have been found useful for clinical application.

There is thus a need for models accounting for the fundamental features of LGG dynamics and their response to radiation therapy without involving excessive details on the -often unknown- specific processes but allowing the qualitative understanding of the phenomena involved. The availability of systematic and quantitative measurements of LGG growth rates provides key information for the development and validation of such models (Pallud *et al.*, 2012a,b).

In this paper, we present a simple mathematical model capturing the key features seen in the response of LGGs to radiation. Our model incorporates the basic elements of tumour dynamics: infiltration and invasion of the normal brain by the tumour cells, proliferation and tumour cell death in response to therapy. Radiation therapy is included in an almost parameter-free way that captures the essentials of the dynamics and explains the relationship between proliferation, response to the therapy and prognosis as recently reported by Pallud *et al.* (2012b).

In addition to explaining the counterintuitive observations of Pallud *et al.* (2012b) the model presented in this paper can be used to explore different radiation regimes. The analysis to be presented in this paper suggests the possibility of using radiation therapy with palliative intent and also to test what the tumour response is and help the oncologists in making the best possible decisions on when and how to act on the tumour.

Our plan in this paper is as follows. First, in Section 2 we present our model accounting for tumour cell dynamics and the response of the tumour cells to radiation. Next in Section 3, we present the results

of the numerical simulations of the model in different scenarios and study the dependence of the model on the different parameters. In Section 4, we display some analytical estimates of the typical dynamics of the tumour response to radiation. In Section 5, we discuss some hypothesis suggested from the model that may be useful for therapy. Finally, in Section 6 we summarize our conclusions.

2. Mathematical model for the response of LGGs to radiotherapy

2.1 *Tumour cell compartment*

In the last years there has been a lot of activity on mathematical models of glioma progression (Stamatakos *et al.*, 2006a,b; Frieboes *et al.*, 2007; Murray, 2007; Swanson *et al.*, 2008; Bondiau *et al.*, 2008; Eikenberry *et al.*, 2009; Tanaka *et al.*, 2009; Wang *et al.*, 2009; Konukoglu *et al.*, 2010; Rockne *et al.*, 2010; Pérez-García *et al.*, 2011; Badoual *et al.*, 2012; Gu *et al.*, 2012; Hatzkirou *et al.*, 2012; Martínez-González *et al.*, 2012; Pérez-García & Martínez-González, 2012; Painter and Hillen, 2013). In this paper, we will consider a model for the compartment of tumour cells of the simplest possible type: a Fisher–Kolmogorov (FK) type equation (Murray, 2007). More complicated models such as single-cell-based models would allow one, in principle, to follow the individual movement of the transformed astrocytes through the brain parenchyma. However, considering that the basic rules behind a model are more important than the model details, we have discarded both the use of on-lattice models, which are not realistic when cell motion is considered, and off-lattice models, which assume fixed cell geometries and/or incorporate unknown cell–cell interactions. Besides, these models often require the estimation of a large number of unknown parameters and the determination of initial cell configurations, which are extremely difficult to validate in *in vivo experiments* and/or using clinical data. Thus, to keep our description as simple as possible, we have opted for a continuous model as follows:

$$\frac{\partial C}{\partial t} = D\Delta C + \rho(1 - C)C, \tag{2.1a}$$

$$C(x, 0) = C_0(x), \tag{2.1b}$$

where $C(x, t)$ is the tumour cell density as a function of time t and the spatial position x and it is measured in units of the maximal cell density allowed in the tissue C_* (typically around 10^3 cell/cm); $\Delta = \sum_{j=1}^{n} \partial^2/\partial x_j^2$ is the n-dimensional Laplacian operator.

By D, we denote the diffusion coefficient accounting for the average cellular motility measured in mm^2/day assumed in this paper to be constant and spatially uniform. Migration in gliomas is not simple and in fact many authors have proposed that the highly infiltrative nature of human gliomas recapitulates the migratory behaviour of glial progenitors (Dirks, 2001; Suzuki *et al.*, 2002). Here we assume, as in most models, that glioma cell invasion throughout the brain is basically governed by a standard Fickian diffusion process. More realistic and complicated diffusion terms in gliomas should probably be governed by fractional (anomalous) diffusion (Fedotov *et al.*, 2011) or other more elaborate terms (Deroulers *et al.*, 2009) to account for the high infiltration observed in this type of tumours (Onishi *et al.*, 2011) and the fact that cells do not behave like purely random walkers and may actually remain immobile for long time periods before being compelled to migrate to a more favourable place. In addition, in real brain there are spatial inhomogeneities expected in the parameter values such as different propagation speeds in white and gray matter, and anisotropies (e.g. on the diffusion tensor with preferential propagation directions along white matter tracts). Many papers have incorporated these details (Clatz, 2005; Jbadi *et al.*, 2005; Bondiau *et al.*, 2008; Konukoglu *et al.*, 2010; Painter and Hillen, 2013) mostly with the intention to make patient-specific progression predictions. However, the main limitation

is the lack of information on the (many) patient-specific unknown details, which has limited progress in that direction. Thus, in order to simplify the analysis and focus on the essentials of the phenomena, we have chosen to study the model in one spatial dimension and in isotropic media. It is interesting that up to now only the simplest models such as those given by Equations (2.1) have been used to extract conclusions useful for clinicians (Swanson *et al.*, 2008; Wang *et al.*, 2009).

The choice of 1D diffusion intends to incorporate qualitatively diffusion phenomena in the simplest possible way. Front solutions of the 1D FK equation have been extensively studied and are known to propagate with a minimal speed $c = 2\sqrt{\rho D}$ when starting from still initial data (Murray, 2007). It is interesting that the 1D model recapitulates the most relevant -for us-phenomenology observed in higher-dimensional scenarios. First, it is obvious and well known that front (invasion wave) solutions of the 1D FK equation also solve higher-dimensional version of the equation (Brazhnik and Tyson, 2000; Xin, 2000). Moreover, those solutions are asymptotically stable (Sattinger, 1976; Xin, 2000), which means that, unlike other more complicated non-symmetrical solutions (Brazhnik and Tyson, 2000), they do arise as limits of non-symmetric initial data. It is also well known that radially symmetric (in 2D) or spherically symmetric (in 3D) travelling wave solutions of FK do not exist in high dimensions but that symmetric fronts also develop in those scenarios with a non-constant speed that depends on the local curvature R (Brazhnik and Tyson, 2000; Volpert & Petrovskii, 2009). As the front grows with time, the now radius-dependent front speed is given by $c(R) = c - D/R(t)$. Thus, growing symmetric multidimensional solutions with large curvature radii ($R \to \infty$) grow with the same speed as 1D fronts (Volpert & Petrovskii, 2009; Gerlee and Nelander, 2012).

In this paper, we are interested on the description of LGGs that typically are very extended when diagnosed, thus the initial data radius is large and fronts are well developed by then. Although during the initial stages of tumour development the dimensionality may play a relevant role, for spatially extended tumours the effect of using higher-dimensional operators is not expected to be substantial.

Moreover, some of the phenomena to be described later in this paper are found to be essentially independent of diffusion and a very good qualitative agreement will be found between our simplified analysis and the growth dynamics of the mean tumour diameter. Taking into account all these evidences, we will keep the system 1D, since our intention is not to provide a detailed quantitative description of the processes -that in any way would be beyond the reach of a simple model such as FK- but instead to provide a qualitative description of the dynamics in the simplest possible way. As we will discuss in detail later, this approach will lead to a simple yet qualitatively correct description of the response of LGGs to radiotherapy.

The parameter ρ in Equation (2.1) is the proliferation rate (1/day), its inverse giving an estimate of the typical cell doubling times. We have chosen a logistic type of proliferation leading to a maximum cell density $C(x, t) = 1$. Finally, the tumour evolves from an initial cell density given by the function $C_0(x)$ in an unbounded domain, so we implicitly assume it to be located initially sufficiently far from the grey matter.

A very interesting feature of model Equations (2.1) is the well-known fact that a tumour front arises propagating at the asymptotic (constant) speed of $v_* = 2\sqrt{D\rho}$, which is in very good agreement with the observed fact that the tumour mean diameter grows at an approximately constant speed (Pallud *et al.*, 2012a).

While many other mathematical models of gliomas incorporate different cell phenotypes, e.g. normoxic (proliferative) and hypoxic (migratory) phenotypes, such as in Martínez-González *et al.* (2012), Hatzkirou *et al.* (2012) and Pérez-García & Martínez-González (2012), here we focus our attention on LGGs and as such will consider a single (dominant) tumour cell phenotype. In our model, we do not include the possible existence of different tumour cell populations with different sensitivities to therapy

such as stem cells, since the function and mechanisms of stem cells in glioblastoma are yet under debate (Barrett *et al.*, 2012; Chen *et al.*, 2012).

2.2 *Response to radiation*

Radiation therapy has been incorporated in different forms to mathematical models of high-grade glioma progression (Barazzuol *et al.*, 2010; Konukoglu *et al.*, 2010; Rockne *et al.*, 2010; Bondiau *et al.*, 2011). In this paper, we want to focus our attention on LGGs whose response to radiation is very different from the one observed in HGGs. Radiation therapy in LGGs typically induces a response that prolongs for several years after therapy.

Very interesting quantitative data on the response of LGGs to radiation have been reported in a retrospective study by Pallud *et al.* (2012a). The authors studied patients diagnosed with grade II LGGs treated with first-line radiotherapy before evidence of malignant transformation. Patients with a post-RT velocity of diametric expansion (VDE) (Pallud *et al.*, 2012a) slower than $-10\,\text{mm/year}$ were taken as a subgroup of slowly growing LGGs. Patients with a post-RT VDE of $-10\,\text{mm/year}$ or faster were included in the group of fast-growing LGGs. The authors concluded that the post-RT VDE was significantly faster in the group with high proliferation. Also, in the patients with an available pre-RT VDE, the low pre-RT VDE subgroup presented a slower VDE at imaging progression. With regard to the ST, post-radiotherapy VDE carried a prognostic significance on ST, as the fast post-radiotherapy tumour volume decrease (VDE at $-10\,\text{mm/year}$ or faster) was associated with a significantly shorter survival than slow post-radiotherapy tumour volume decrease (VDE slower than $-10\,\text{mm/year}$).

The very slow response to radiotherapy, leading to tumour regression lasting for several years is difficult to understand in the context of the standard linear quadratic model in which damage is instantaneous and leads to cell death early after radiation therapy. However, a key aspect of the cell response to radiation is that irradiated cells usually die because of the so-called mitotic catastrophe after completing one or several mitosis cycles (Van der Kogel & Joiner, 2009). This means that slowly proliferating tumours, as in the case of LGGs with typical low proliferation indexes between 1% and 5% in pathological analyses, need a very long time to manifest the accumulated cell damage that cannot be repaired.

Thus, in order to capture in a minimal way the response of the tumour to radiation, we will complement Equation (2.1) for the density of functionally alive tumour cells $C(x, t)$ with an equation for the evolution of the density of irreversibly damaged cells after irradiation $C_d(x, t)$. Our model for the evolution of both tumour cell densities will be given by the equations

$$\frac{\partial C}{\partial t} = D\Delta C + \rho(1 - C - C_d)C, \tag{2.2a}$$

$$\frac{\partial C_d}{\partial t} = D\Delta C_d - \frac{\rho}{k}(1 - C - C_d)C_d. \tag{2.2b}$$

The first equation is a Fisher–Kolmogorov-type equation describing the evolution of tumour cells $C(x, t)$. The saturation term includes the total tumour cell density, i.e. both the functional tumour cells and those damaged by radiation $C_d(x, t)$. The evolution of cells irreversibly damaged by radiation is given by Equation (2.2b). As is well described in the literature (Van der Kogel & Joiner, 2009), most of these cells behave normally until a certain number of mitosis cycles; thus we will consider that, after an average of k mitosis cycles, these cells die resulting in a negative proliferation. The longer ST $k\tau$, with $\tau = 1/\rho$ being the tumour population doubling time, results in a reduced proliferation potential ρ/k, which is the coefficient used for the negative proliferation term. Thus, the parameter k in Equation (2.2b) has the meaning of the average number of mitosis cycles that damaged cells are able to

complete before dying. As with the normal population, the number of cells entering mitosis depends in a non-linear way on both tumour cell populations (cf. last term in Equation (2.2b)).

We will assume a series of radiation doses $d_1, d_2, \ldots, d_n$ given at times $t_1, t_2, \ldots, t_n$. The initial data for the first subinterval will be given by the equations

$$C(x, t_0) = C_0(x), \tag{2.3a}$$

$$C_d(x, t_0) = 0. \tag{2.3b}$$

The evolution of the tumour follows then Equations (2.2) until the first radiation dose d_1, given at time t_1. The irradiation results in a fraction of the cells (surviving fraction) able to repair the radiation-induced damage given by $S_f(d_1)$ and a fraction $1 - S_f(d_1)$ of cells unable to repair the accumulated damage, thus feeding the compartment of irreversibly damaged cells. The subsequent evolution of the populations is again given by Equations (2.2) until the next RT dose is given. In general, after each irradiation event we obtain

$$C(x, t_j^+) = S_f(d_j)C(x, t_j^-), \tag{2.3c}$$

$$C_d(x, t_j^+) = C_d(x, t_j^-) + [1 - S_f(d_j)]C(x, t_j^-), \tag{2.3d}$$

where $S_f(d_j)$ is the survival fraction after a dose of radiation d_j, i.e. the fraction of damaged tumour cells after irradiation that are not able to repair lethal damage and are incorporated to the compartment of damaged cells. For the doses to be considered independent, the interval between doses (typically 1 day) has to be larger than the typical damage repair times (of the order of hours). The evolution of both cell densities between irradiation events is given by the partial differential equations (PDEs) (2.2).

2.3 *Parameter estimation*

Equations (2.2) together with the initial conditions for each subproblem (2.3) define completely the dynamics of an LGG in the framework of our simplified theoretical approach.

We have chosen the parameters to describe the typical growth patterns of LGG. For the proliferation rate we have chosen typical values to be small and around $\rho = 0.003$ day^{-1} (see e.g. Badoual *et al.*, 2012), which give doubling times of the order of a year. Specifically, we have considered values ranging from $\rho = 0.001$ day^{-1} for very slowly growing LGGs to $\rho = 0.01$ day^{-1}. For the cell diffusion coefficient we have taken values around $D = 0.0075$ mm^2/day (Jbadi *et al.*, 2005). This choice, together with the previously chosen ρ, leads to asymptotic tumour diameter growth speeds given by $v = 4\sqrt{D\rho}$ of the order of several millimetres per year, in agreement with typical diametric growth speeds of LGGs (Pallud *et al.*, 2012a). However, the fact that the asymptotic speed is only reached when the tumour cell density is around 1 may require taking larger values of D to match the real growth speeds.

With regards to the radiobiological parameters, gliomas being very resistant to radiation, we have taken values in the range $S_f(1.8\,\text{Gy}) \equiv \text{SF}_{1.8} \sim 0.9$ considering the median survival fraction value 0.83 after one dose of 2 Gy given by Barazzuol *et al.* (2010) .

Finally, the average number of mitosis cycles completed before the mitotic catastrophe occurs is difficult to estimate. This parameter intends to summarize in a single number a complex process in which a cell hit by radiation and its progeny die after some more mitosis cycles leading to a final extinction after a variable time. Death by mitotic catastrophe implies a minimal value of $k = 1$ and, to allow for some more time, we may choose values in the range $k = 1 - 3$ (Van der Kogel & Joiner, 2009). We will show later that the choice of this parameter has a limited effect on the model dynamics and that, in standard fractionation schemes, there may be biological reasons to take it as $k = 1$.

TABLE 1 *Typical values of the biological parameters in the model of LGG evolution*

Variable	Description	Value (Units)	References
C_*	Maximum tumour cell density	10^6 cell/cm^2	Swanson *et al.* (2008)
D	Diffusion coefficient for tumour cells	0.01 mm^2/day	Jbadi *et al.* (2005)
ρ	Proliferation rate	0.00356 day^{-1}	Badoual *et al.* (2012)
$SF_{1.8}$	Survival fraction for 1.8 Gy	~0.9	Barazzuol *et al.* (2010)
k	Average number of mitosis cycles completed before the mitotic catastrophe	1–3	Van der Kogel & Joiner (2009)

Our typical choices for the full set of model parameters is summarized in Table 1.

In this paper, we will fix the dose per fraction in agreement with the standard fractionation schemes for LGGs to be 1.8 Gy; the only relevant parameter is the survival fraction $SF_{1.8}$, which will be taken to be around $SF_{1.8} \sim 0.9$, as discussed above. In many examples, we will choose the radiotherapy scheme as the standard fractionation of a total of 54 Gy in 30 fractions of 1.8 Gy over a time range of 6 weeks (5 sessions per week from Monday to Friday).

3. Results

3.1 *Computational details*

We have studied the evolution of the tumour diameter using our model Equations (2.2) and (2.3). To solve the PDEs we have used standard second order finite differences both in time and space. Since the tumour diameter in the framework of this model tends to grow linearly in any spatial dimension we have focused on the simplest 1D version of the model. We have checked with simulations in higher dimensions that the dynamics is essentially the same and thus have sticked to the simplest possible model. To avoid boundary effects and focus on the bulk dynamics, we have assumed our computational domain to be much larger than the tumour size.

In each simulation, we have computed the tumour diameter as the distance between the points for which the density reaches a critical detection value C_{th} that provides a signal in the T2 (or FLAIR) MRI sequence. Although which is that precise value is a debated question and in fact depends on the thresholds used in the images, we have assumed that $C_{th} \sim 0.05 - 0.07$. This is in agreement with the reported value of cellular density about 0.16 for detection (Swanson *et al.*, 2008) and a normal tissue density of about 0.1. In agreement with previous studies we take a fatal tumour burden (FTB) size of 6 cm in diameter (Swanson *et al.*, 2008; Wang *et al.*, 2009). As parameters containing useful information we have computed: the time in which the tumour starts regrowing after the therapy, usually called in clinical practice time to tumour progression (TTP), the time for which the tumour size equals its initial size -denoted as growth delay (GD)- and the time for which the tumour size equals the FTB or ST.

We have studied a broad range of parameter values corresponding to the possible range of realistic values in the framework of our simple description of the tumour dynamics and its response to radiotherapy. We have also taken different types of initial data ranging from more localized (such as gaussian initial profiles) to more infiltrative (such as sech-type functions). In what follows, we summarize our results.
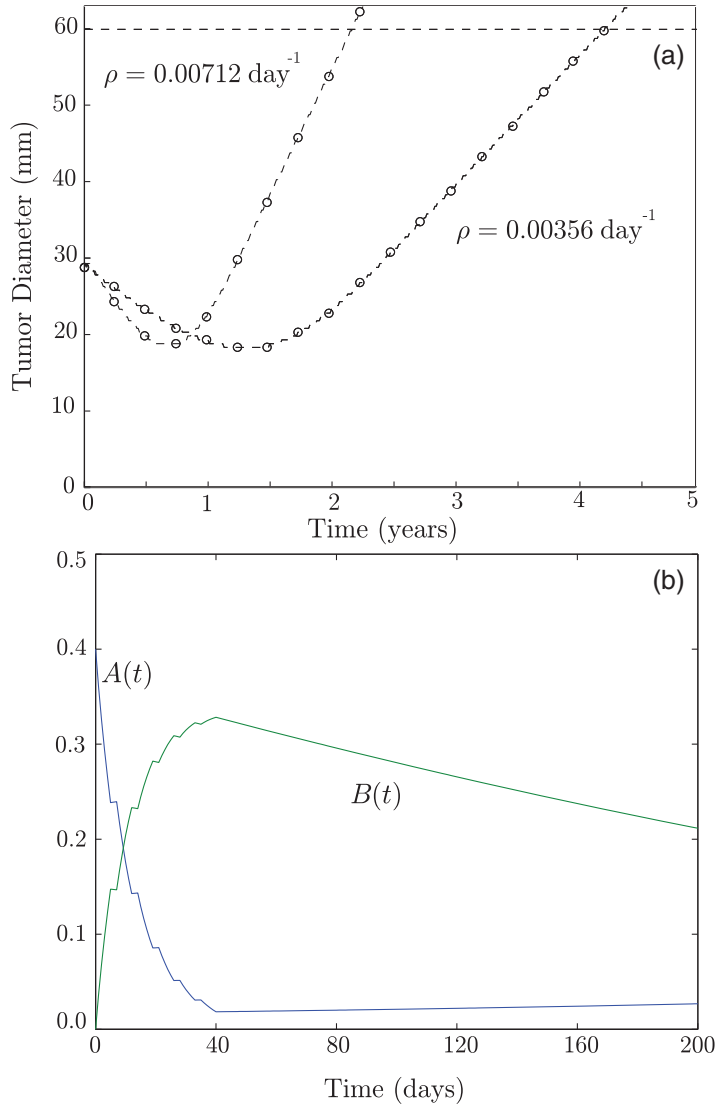
FIG. 1. (a) Tumour diameter evolution for two different values of the proliferation: $\rho = 0.00356$ day^{-1}, $\rho = 0.00712$ day^{-1}. Other parameter values are: $D = 0.0075$ mm^2/day, critical detection value $C_{th} = 0.07$, SF$_{1.8} = 0.90$ and $k = 1$. The initial tumour cell densities are taken as $C_d(x, 0) = 0$, $C(x, 0) = 0.4$ sech$(x/6)$, with x measured in millimetres, which gives an initial tumour diameter of 28.8 mm. Radiotherapy follows the standard scheme (6 weeks with 1.8 Gy doses from Monday to Friday) and starts at time $t = 0$. Circles denote measurements every three months that would correspond to a close follow-up of the patient. The upper dashed line (horizontal) shows the FTB size taken through this paper to be 6 cm, as discussed in the text. (b) Evolution of the tumour cell amplitudes $A(t) = \max_x |C(x, t)|$ and $B(t) = \max_x |C_d(x, t)|$ during the first 200 days showing the early response to the therapy for $\rho = 0.00356$ day^{-1}.

3.2   *Tumour proliferation rate determines the response to radiotherapy*

In a first series of simulations, we have studied the dependence of the evolution of the tumour diameter on the proliferation rate. Figure 1(a) shows the evolution of the tumour diameter for two different

proliferation rates $\rho = 0.00356$ day^{-1} and $\rho = 0.00712$ day^{-1} (Fig. 1). In the first case of low prolif-eration, the tumour responds more slowly to therapy as measured by the speed of tumour regression (decrease in size) but the total response time is significantly longer, the TTP being 16.9 months against 8.2 months in the later case. Also the GDs is 14.7 months for the faster proliferating tumour against 29.9 months for the less proliferative one. Finally the 'virtual patient' with the slowly proliferating tumour survives much longer than that with the more proliferative one. This is just an example of a tendency shown in all of our simulations where 'more aggressive tumours respond earlier to the therapy'.

It is remarkable that this fact is in full agreement with the results from Pallud *et al.* (2012b). Our model based on reasonable biological assumptions leads to a long remission time (e.g. in Fig. 1 of about 3 years), much larger than the treatment duration (6 weeks) and negatively correlated with the tumour proliferation rate. As a second relevant finding, also seen in the results shown by Pallud *et al.* (2012b), we observe that tumours responding faster have also shorter re-growth time.

Figure 1(b) shows the dynamics of the maximum density of tumour cells ($A(t) = \max_x C(x, t)$) and damaged tumour cells ($B(t) = \max_x C_d(x, t)$). As could be expected, the amplitude of functionally alive tumour cells decreases during the therapy with the exception of the breaks in the weekends when a small increase is seen and correspondingly the amplitude of damaged tumour cells grows after every irradiation and for the full treatment period (6 weeks = 42 days). After $t = 42$ days the population of tumour cells starts a slow recovery, while the population of damaged cells declines in a much longer time scale. However, the width of the total tumour population evolves only in the slow time scale and does not display any effects during the treatment period.

It is important to emphasize that this behaviour is not the result of a fortunate choice of the parameters but a generic behaviour as we have confirmed through a large number of simulations covering the full clinically relevant parameter space. As an example, in Fig. 2 we show how the variation of ρ over a broad range of values leads to the same conclusion. Larger proliferation values accelerate the response but lead to earlier re-growth and, as such, shorter GDs and STs (Fig. 2(a)). Our simulations also point out that the maximum volume reduction is only weakly dependent on the proliferation rate ρ (Fig. 2(b)), the smaller the proliferation rates the larger being the maximum reduction in diameter. This fact is also in very good agreement with the results of Pallud *et al.* (2012b) (see e.g. Fig. 2 bottom of their paper).

3.3 *The role of the number of mitosis cycles before clonogenic cell death*

It is well known that most cells die after irradiation through the so-called mitotic catastrophe, i.e. due to incomplete mitosis, after completing one or several mitosis cycles. However, the specific choice of the parameter k is not a priori obvious although a number between one and three is to be expected a priori from previous experience in vitro (Van der Kogel & Joiner, 2009). To get some information on how our model's results depend on this parameter, we have explored numerically the range $k = 1$–3.

Our results are summarized in Fig. 3. First, in Fig. 3(a) we show typical evolutions of the tumour diameter for three different values of $k = 1$ (triangles), $k = 2$ (squares) and $k = 3$ (circles) for $\rho = 0.00712$ day^{-1}. It is clear that although the diameter reduction depends on k (Fig. 3(b)), the specific choice of this parameter does not affect the more relevant parameters such as the GD and the total sur-vival (see Fig. 3(a,c)). From this and other simulations, we think the specific choice of this parameter does not have a crucial role on the dynamics of clinically relevant features.

In addition, although in vitro irradiation of cells with a single dose allows cells to complete a few mitosis cycles, the accumulation of many doses in real treatment schedules implies that a typical cell receives a lot of DNA damage. This will probably make it very difficult for cells in vivo to progress after the first mitosis, thus making it reasonable to take $k = 1$. This fact, together with the previous result
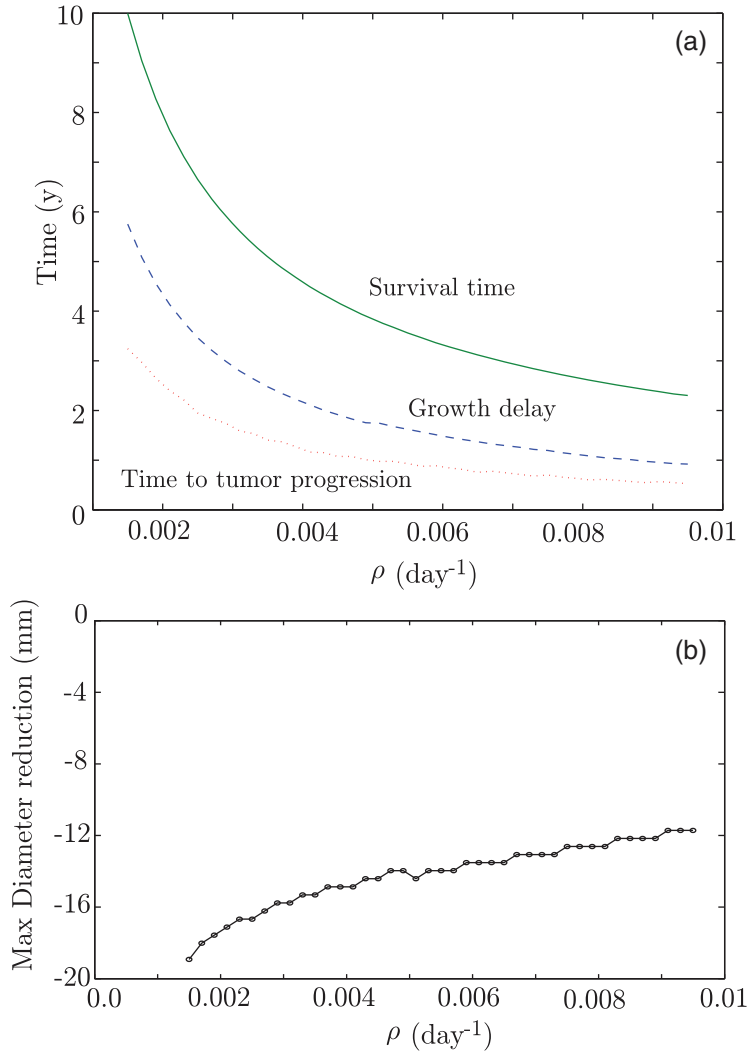
FIG. 2. Dependence of the (a) ST (solid line), GD (dashed line), TTP (dotted line) and (b) maximal reduction in diameter as a function of ρ. The curves summarize the outcome of many individual simulations with initial data $C_d(x, 0) = 0, C(x, 0) = 0.2 \exp(-x^4/81920)$, with x measured in millimetres, which gives an initial tumour diameter of 33.80 mm. Radiotherapy follows the standard scheme (6 weeks with 1.8 Gy doses from Monday to Friday) and starts at time $t = 0$. Other parameters used in the simulations are as in Fig. 1.

on the independence of the clinically relevant endpoints on k makes the choice of $k = 1$ a reasonable assumption not expected to have a relevant impact on the final results.

3.4   *The role of cell motility*

We have also analysed the role of the variation of the cell motility (invasion) parameter D. The typical outcome of several simulations for different values of this parameter is shown in Fig. 4. It is clear from Fig. 4(a) that cell motility does not affect too much the dynamics of the response to the therapy except
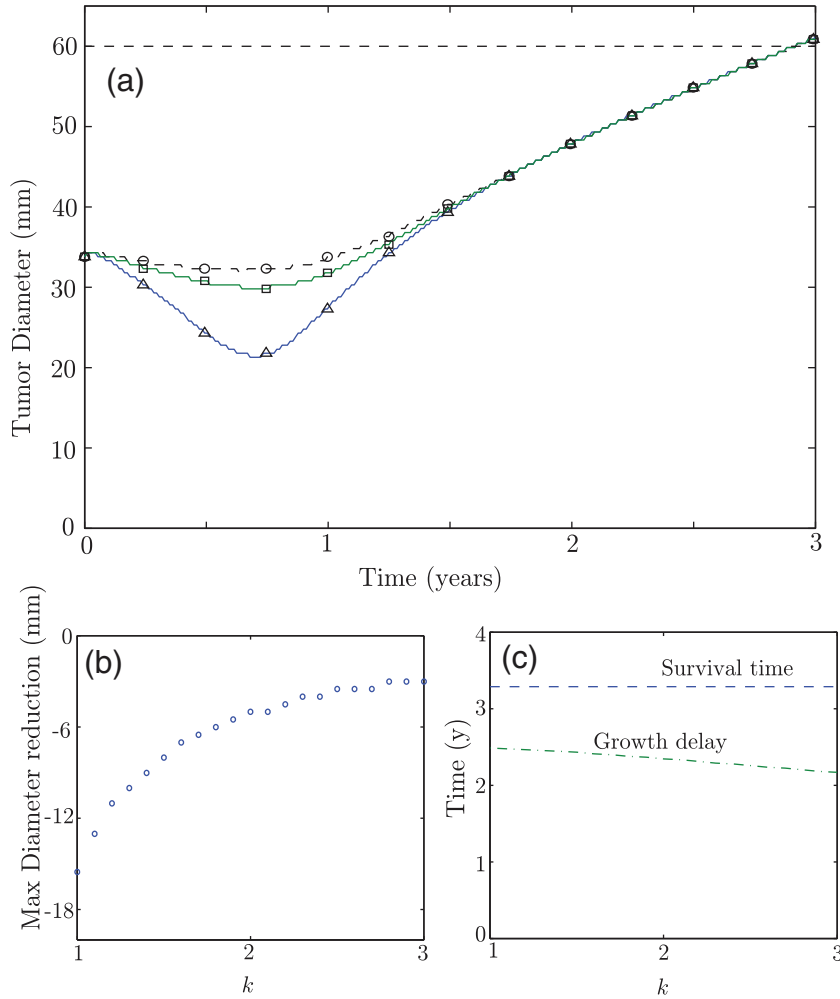
FIG. 3. (a) Tumour diameter evolution for three different values of $k = 1$ (triangles), $k = 2$ (squares) and $k = 3$ (circles) for $\rho = 0.00712$ day^{-1}. Other parameters are as in Fig. 2. The upper dashed line (horizontal) corresponds to the FTB size. Radiotherapy follows the standard scheme (6 weeks with 1.8 Gy doses from Monday to Friday) and starts at time $t = 0$. It is clear that, for this set of parameters, the ST does not depend on k despite the differences in the maximum diameter reduction achieved by the therapy. (b) Maximum diameter reduction for different values of the mean number of mitosis cycles completed before cell death with k between 1 and 3. (c) ST and GD as a function of k.

for long times because of the effect of the mobility on the asymptotic VDE $v = 4\sqrt{\rho D}$. This manifests in the independence of the TTP and GD on D and the relevant impact of this parameter on the ST (Fig 4(b)).

3.5 *Deferring radiotherapy does not affect ST*

One clinical fact on radiotherapy of LGGs that has been proved in the last years is that deferring radiotherapy has no significant impact on the ST (Bauman *et al.*, 1999; Van den Bent, 2005). To test if our
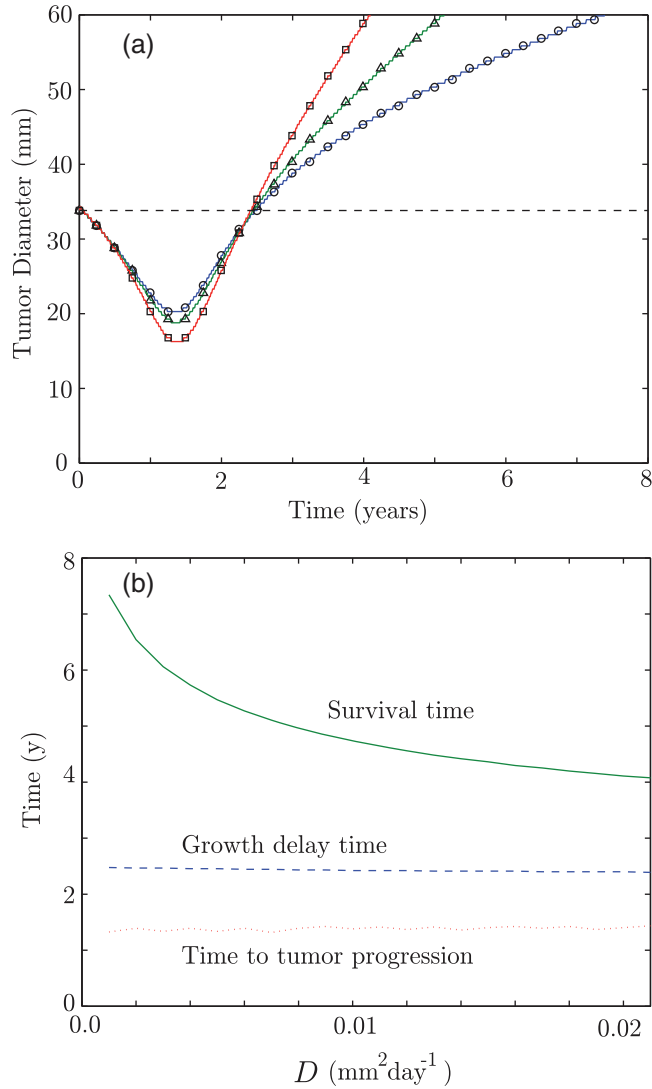
FIG. 4. (a) Tumour diameter evolution for three different values of $D = 0.001 \, \text{mm}^2\text{day}^{-1}$ (circles), $D = 0.007 \, \text{mm}^2\text{day}^{-1}$ (triangles) and $D = 0.021 \, \text{mm}^2\text{day}^{-1}$ (squares) for $\rho = 0.00356 \, \text{day}^{-1}$. Other parameters and initial data are as in Fig. 2. Radiotherapy follows the standard scheme (6 weeks with 1.8 Gy doses from Monday to Friday) and starts at time $t = 0$. It is clear that, for this set of parameters, the early response to the therapy does not depend on D, while the asymptotic growth does (b) ST, GD and TTP as a function of D. Only the ST depends substantially on the cell motility D.

model presents this behaviour, we have run several series of simulations with different delays in the start of the radiotherapy and compared the outcome. Typical results are shown in Fig. 5. The results of the model fully agree with this very well-known fact, which gives us more confidence in the model's predictive power, despite its simplicity.
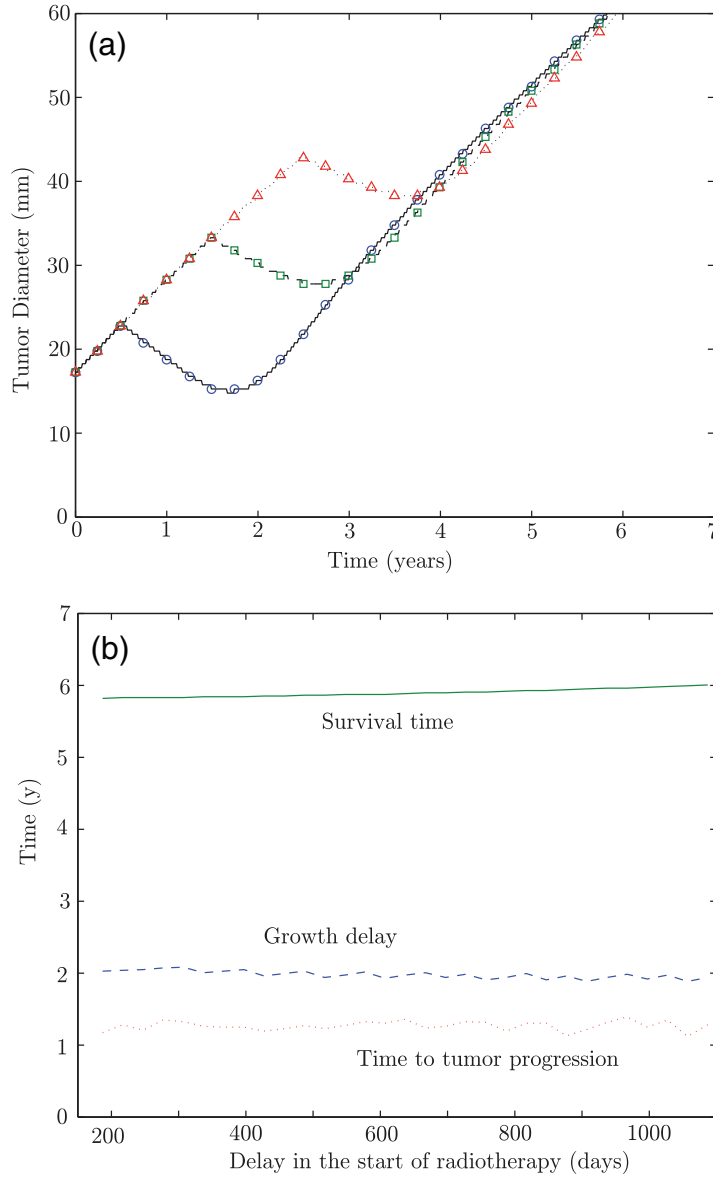
FIG. 5. Evolution of an initial tumour density given by $C(x, 0) = 0.2 \exp(-x^2/(2w^2))$, $C_d(x, 0) = 0$ for $w = 6$, with (x, w) being measured in millimetres, and parameter values $D = 0.01$ mm^2/day, $\rho = 0.004$ day^{-1}, SF$_{1.8} = 0.9$ and $k = 1$. Radiotherapy follows the standard scheme (6 weeks with 1.8 Gy doses from Monday to Friday) and starts at a given time T_{RT} after the beginning of the simulation for $t = 0$. Shown are (a) Tumour diameter evolution for three different values of $T_{RT} = 6$ months (solid line, circles), $T_{RT} = 18$ months (dashed line, squares), $T_{RT} = 30$ months (dotted line, triangles). (b) ST (solid line), GD (dashed line) and TTP (dotted line) as a function of the delay T_{RT} in the start of radiotherapy.
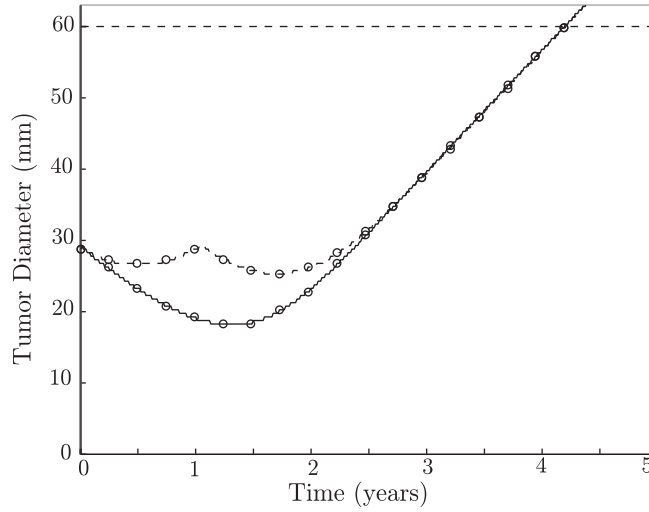
FIG. 6. Tumour diameter evolution for parameter values $D = 0.007$ mm^2/day, $\rho = 0.00356$ day^{-1}, initial data as in Fig. 1 and two different fractionations of the total dose. The solid line corresponds to the tumour evolution under 30 doses of 1.8 Gy given from Monday to Friday for six consecutive weeks starting 1 week after $t = 0$. The dashed line corresponds to the tumour diameter evolution under the same fractionation scheme for the first three weeks and then deferring the remaining 15 doses for 1 year. Despite the time of response being shorter, the final ST is the same in both fractionation schemes.

3.6   *Splitting doses does not affect ST*

We have studied the response of the tumour to radiotherapy under many different fractionation schemes, maintaining the dose per fraction to be 1.8 Gy. Surprisingly, all of the studied fractionations lead to very similar results for the virtual patient's ST. A typical example is shown in Fig. 6.

Although we have not tried every possible combination, this fact points out the difficulty of constructing specific fractionation schemes leading to a better outcome than those currently in use. However, the results of Fig. 6 have interesting potential practical applications as will be discussed in Section 5.

4. Some analytical estimates

The model equations given by Equations (2.2), though simple, do not have known analytical solutions allowing for the direct calculation of the clinically relevant quantities, i. e. the TTP (t_{TTP}), the GD (t_{GD}) and the time to FTB. Even for the simplest version of the Fisher–Kolmogorov equations only a limited number of solutions are known for specific parameter values (Ablowitz & Zeppetella, 1979; Murray, 2007).

Here, we present some back-of-the-envelope calculations that may help in getting a qualitative idea of the typical dynamics of the tumour response to radiation. The basic idea behind our estimates is that, during some time after irradiation, the dominant component of the dynamics is the refilling of the compartment of the proliferating tumour cells, and diffusion acts on a longer time scale, being responsible for the asymptotic front speed (see e.g. Fig. 4(a)) but having only a negligible influence both on the TTP and the GD (Fig. 4(b)).

We will assume the tumour densities shortly after irradiation to be small enough to allow for the non-linear terms to be neglected (it is in agreement with the low cellularity characteristic in LGG histologic samples). This is obviously true for the tumour compartment whose typical cell densities after irradiation are small until the tumour refills the space. With regard to the damaged tumour cell compartment its maximal density is of the order of the maximal initial tumour cell density (about 0.3–0.4) but decays in space to smaller cell densities and will be assumed to contribute only through the leading linear terms.

As a final assumption, we will assume the total treatment time to be short in comparison with the typical proliferation times so that the effect of the radiotherapy will be incorporated through a modification of the pretreatment tumour cell density $C_0(x)$. Thus, for our rough estimates we will take

$$C(x,0) = S_f^n C_0(x), \tag{4.1a}$$

$$C_d(x,0) = (1 - S_f^n)C_0(x). \tag{4.1b}$$

Our set of hypothesis leads to a very simple evolution law for the total densities, valid for short times:

$$C(x,t) \approx S_f^n C_0(x)\, e^{\rho t}, \tag{4.2a}$$

$$C_d(x,t) \approx (1 - S_f^n)C_0(x)\, e^{-\rho t/k}, \tag{4.2b}$$

so that, for some time after the therapy, the total tumour cell density $C_T(x,t)$ can be roughly approximated by

$$C_T(x,t) \approx [S_f^n\, e^{\rho t} + (1 - S_f^n)\, e^{-\rho t/k}]C_0(x), \tag{4.3}$$

where $A(t) \equiv S_f^n\, e^{\rho t} + (1 - S_f^n)\, e^{-\rho t/k}$ provides an estimate of the tumour maximum density as a function of time. From this simple formula, we can estimate the GD time since it would correspond to the time $t_{GD} > 0$ such that

$$S_f^n\, e^{\rho t_{GD}} + (1 - S_f^n)\, e^{-\rho t_{GD}/k} \approx 1. \tag{4.4}$$

Although Equation (4.4) is an algebraic equation with no simple explicit solutions by the time re-growth occurs, we can expect the first term to have a very small contribution, while the second one would dominate, which gives

$$t_{GD} \approx \frac{1}{\rho} \log\left(\frac{1}{S_f^n}\right) \approx \frac{n(1 - S_f)}{\rho}. \tag{4.5}$$

This equation incorporates the fact that the GD time does not depend much on the diffusion parameter D (see e.g. Fig. 4(b)), nor on the number of mitosis cycles before cell death for damaged cells (see e.g. Fig. 3(c)), and points out a direct simple dependence of this time on the survival fraction, number of doses and proliferation parameter. Moreover, the dependence of t_{GD} on ρ is $\sim 1/\rho$, which resembles closely the dependence depicted in Fig. 2. We can also get estimates for the TTP since it corresponds to the point of minimum amplitude, corresponding to the time t_{TTP} such that $A'(t_{TTP}) = 0$,

$$\frac{d}{dt}[S_f^n\, e^{\rho t} + (1 - S_f^n)\, e^{-\rho t/k}] = 0, \tag{4.6}$$

which leads to

$$t_{TTP} = \frac{1}{\rho(1 + 1/k)} \log\left(\frac{1 - S_f^n}{S_f^n}\right) \simeq \frac{n(1 - S_f)}{\rho(1 + 1/k)} \tag{4.7}$$
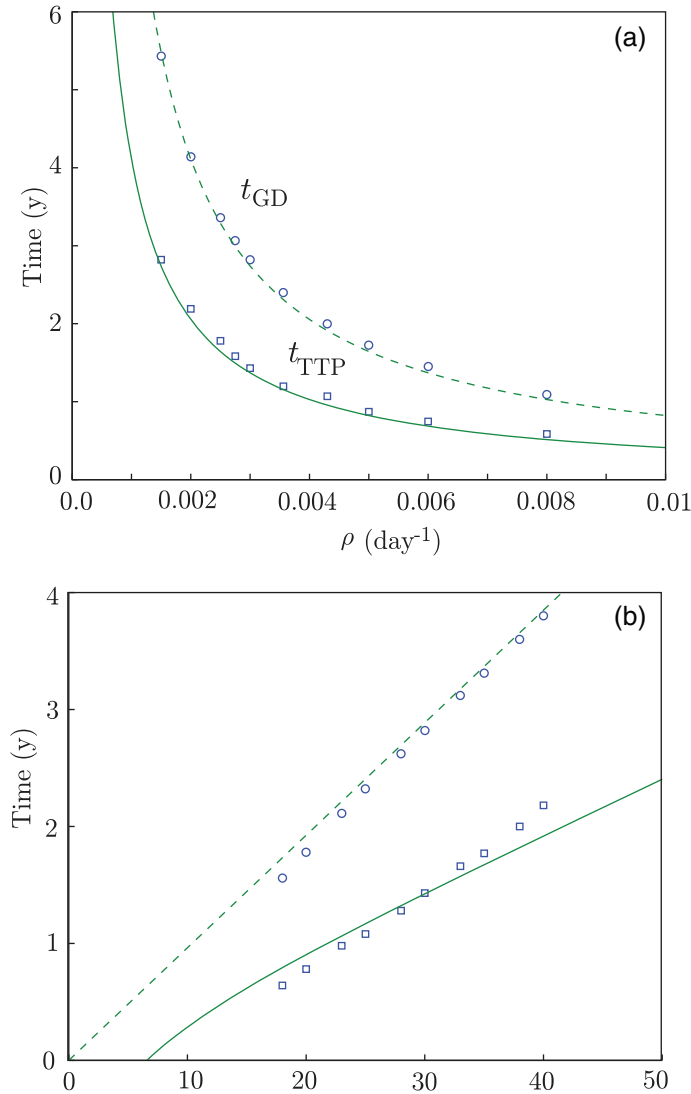
FIG. 7. Comparison of the estimates for t_{GD} (circles) and t_{TTP} (squares) obtained from Equations (4.5) and (4.7) and their exact values (lines) obtained from numerical simulations of Equations (2.2) in different scenarios. In all cases $D = 0.007 \, \text{mm}^2/\text{day}$, $S_f = 0.9$ and $k = 1$ and initial data are as in Fig. 1. (a) Dependence on the proliferation parameter ρ for a fixed number of doses $n = 30$ following the standard fractionation scheme. (b) Dependence on the number of doses n for fixed $\rho = 0.002 \, \text{day}^{-1}$.

While these estimates are obtained as rough approximations for the response to radiation, they provide a very reasonable agreement with the results of direct numerical simulations of Equations (2.2). For instance, in Fig. 7(a), we compare the results for the GD and TTP provided by Equations (4.5) and (4.7) with the results from Equations (2.2) for a typical set of parameters and varying the proliferation parameter ρ. In Fig. 7(b), we compare the predictions for t_{TTP} and t_{GD} given by Equations (4.5) and (4.7) for different values of the number of radiation fractions n, with the simulations of the full PDEs.

In addition to these quantities, it is possible to use Equation (4.3) to get estimates for the conditions of response to therapy ($A'(0) < 0$), i.e.

$$A'(0) = \rho S_f^n - \rho(1 - S_f^n)/k < 0. \tag{4.8}$$

This leads to the result that an estimate for the minimal number of doses leading to a response is about

$$n > -\frac{\log(1 + k)}{\log S_f}. \tag{4.9}$$

Interestingly, this number is independent of ρ and, for the typical values of S_f used in our simulations, we get a minimal number of sessions around 7 and 9. We have compared this estimate with the results of direct simulations of Equations (2.2) and found a very good agreement. For instance, taking typical initial data and parameter values $C(x, 0) = 0.4 \operatorname{sech}(x/11)$, $\rho = 0.00356 \, \text{day}^{-1}$, $k = 1$, $D = 0.0075 \, \text{mm}^2/\text{day}$ and $S_f = 0.92$, we get a response for $n \geqslant 10$ that is very close to the theoretical estimate computed from Equation (4.9), which is $n \geqslant 9$. The same happens for other parameter choices.

Finally, neither the GD as given by Equation (4.5) nor the TTP (4.7) depends on the initial amplitude or time t_0. This means that radiation can be deferred with no effect on these quantities, which matches very well the behaviour observed in Fig. 5(b).

5. Discussion and therapeutical implications

The intention of this paper is to propose a simple mathematical model adding radiation therapy in a minimal way to the simplest model of tumour progression. Despite its simplicity, the model reproduces many of the well-known facts of RT of LGGs as well as the recent results by Pallud *et al.* (2012b). The fact that the model reproduces so well what is known makes us wonder if it can be used to obtain any new information and/or to propose novel ideas with the potential of translational application. In this section we make several proposals based on the mathematical model.

The first one is based on the fact, discussed in Section 3.6, that deferring part of the treatment does not affect ST. This concept opens the door to dose fractionation approaches where part of the radiation is given right after surgery as an adjuvant therapy and the remaining radiation is given on progression (or later), thus controlling early the tumour while deferring in time the appearance of side effects. A specific way of implementing this idea would be to complete the radiation therapy exactly when the tumour size is minimal so that the irradiated volume is substantially smaller than initially and the side effects due to the so-called volume effect would be reduced. Thus, instead of waiting till the tumour has extended substantially, the first dose would be given right after resection and the second one on minimal volume. The fact that the tumour volume irradiated would be smaller might allow for the consideration of dose escalation protocols while maintaining the side effects under control.

A second implication of our model is that delivery of a reduced radiation dose larger than the minimal response dose (e.g. 30 Gy) should have a verifiable effect on tumour size. Monitoring the response of the tumour to radiation, one could get an idea of its malignancy due to the relation between response time and proliferation, and correlate the finding with the proliferation index obtained through immunohistochemistry when available. The toxicity of this approach for the normal brain is low since 30 Gy is about the same level of the prescriptions for even full-brain irradiation under metastatic spreading, a dose that is very well tolerated by the brain.

Having an early estimate of the tumour aggressiveness is a potentially interesting information since, in addition to making survival estimates (from the tumour parameters ρ, D), it would allow to discriminate tumours that are not as benign as initially thought. A first reason is that the tumour may have transformed to some degree into a more malignant one. This happens sometimes when the histological analysis is old, and by the time RT starts the tumour has become malignant. A different relevant source of error on diagnosis is sampling error if the histology was obtained through biopsy. In fact, biopsy is known to underestimate glioma grade in roughly 30% of cases (Muragaki *et al.*, 2008) due to localized malignant transformation outside the biopsy location. Those tumours with high proliferation values obtained from the mathematical modelling should be expected to have early (radiological) malignant transformation and then MRIs should be taken at shorter intervals, as suggested e.g. by Pallud *et al.* (2012b) for fast-growing tumours. A final therapeutic option for those tumours with fast growth and/or expected early malignant transformation should be to consider another surgery (if feasible) or to start chemotherapy.

Thus, taking together our two ideas, we could make specific recommendations: for tumours with a high risk of malignant transformation, i.e. short re-growth time, our suggestion would be to complete the full radiation dosing, while for those growing slowly one could wait either until the malignant transformation or to the point where the tumour starts re-growing.

6. Conclusions

In conclusion, in this paper we have constructed a mathematical model combining the standard Fisher–Kolmogorov dynamics for tumour cells with a model for the response to radiation based on radiobiological facts. Our equations provide a theoretical link between proliferation and response to therapy, which is one of the main results of this paper. The model predicts that tumours with high proliferation will respond faster to RT than those with slower proliferation values. However, this regression would only be transient and a regrowth is expected early in those tumours responding faster. This fact, despite being somewhat counterintuitive, has been confirmed in very recent retrospective studies by Pallud *et al.* (2012b). The model also displays the observed behaviour that deferring RT does not affect ST.

The equations allow one to obtain analytical estimations for the GD time, TTP and conditions of response to therapy such as the minimal number of doses leading to a response.

In addition to describing the known features of the response of LGGs to radiotherapy, the model allows one to get interesting predictions that may be amenable to further research. One of them is to follow a split-dose approach with a fraction of the total amount of radiation being given after surgery and the remaining on progression. This methodology would allow one to get information on the tumour growth parameters that may lead to estimates of the expected time to malignant transformation, survival, etc., while at the same time reducing toxicity.

We hope that our results will stimulate further collaborative studies directed to improve the quality of life of patients suffering from this devastating disease.

REFERENCES

ABLOWITZ, M. J. & ZEPPETELLA, A. (1979) Explicit solutions of Fisher's equation for a special wave speed. *Bull. Math. Biol.*, **41**, 835.

BARAZZUOL, L., BURNET, N. G., JENA, R., JONES, B., JEFFERIES, S. J. & KIRKBY, N. F. (2010) A mathematical model of brain tumour response to radiotherapy and chemotherapy considering radiobiological aspects. *J. Theor. Biol.*, **262**, 553–565.

BARRETT, L. E., GRANOT, Z., COKER, C., IAVARONE, A., HAMBARDZUMYAN, D., HOLLAND, E. C., NAM, H. S. & BENEZRA, R. (2012) Self-renewal does not predict tumor growth potential in mouse models of high-grade glioma. *Cancer Cell*, **21**, 11–24.

BAUMAN, G., PAHAPILL, P., MACDONALD, D., FISHER, B., LEIGHTON, C. & CAIRNCROSS, G. (1999) Low grade glioma: a measuring radiographic response to radiotherapy. *Can. J. Neurol. Sci.*, **26**, 18–22.

BONDIAU, P. Y., FRENAY, M. & AYACHE, N. (2008) Biocomputing: numerical simulation of glioblastoma growth using diffusion tensor imaging. *Phys. Med. Biol.*, **53**, 879–893.

BONDIAU, P. Y., KONUKOGLU, E., CLATZ, O., DELINGETTE, H., FRENAY, M. & PAQUIS, P. (2010) Biocomputing: numerical simulation of glioblastoma growth and comparison with conventional irradiation margins. *Phys. Med.*, **27**, 103–108.

BRAZNHNIK, P. K. & TYSON, J. J. (2000) On traveling wave solutions of Fisher's equation in two spatial dimensions. *SIAM J. Appl. Math.*, **60**, 371–391.

CHEN, J., LI, Y., YU, T. S., MCKAY, R. M., BURNS, D. K., KERNIE, S. G. & PARADA, L. F. (2012) A restricted cell population propagates glioblastoma growth after chemotherapy. *Nature*, **488**, 522–526.

CLATZ, O., SERMESANT, M., BONDIAU, P. Y., DELINGETTE, H., WARFIELD, S. K., MALANDAIN, G. & AYACHE, N. (2005) Realistic simulation of the 3-D growth of brain tumors in MR images coupling diffusion with biomechanical deformation. *IEEE Trans. Med. Imaging*, **24**, 1334–1346.

DEROULERS, C., AUBERT, M., BADOUAL, M. & GRAMMATICOS, B. (2009) Modeling tumor cell migration: From microscopic to macroscopic models. *Phys. Rev. E*, **79**, 031917.

DIRKS, P. B. (2001). Glioma migration: clues from the biology of neural progenitor cells and embryonic CNS cell migration. *J. Neurooncol.*, **53**, 203–212.

EIKENBERRY, S. E. & KUANG, Y. (2009). Virtual glioblastoma: growth, migration and treatment in a three-dimensional mathematical model. *Cell Prolif.*, **42**, 511–528.

FEDOTOV, S., IOMIN, A. & RYASHKO, L. (2011) Non-Markovian models for migration-proliferation dichotomy of cancer cells: Anomalous switching and spreading rate. *Phys. Rev. E*, **84**, 061131.

FRIEBOES, H. B., BEARER, E. & CRISTINI, V. (2007). Computer simulation of glioma growth and morphology. *Neuroimage*, **37**, S59–S70.

GARCIA, D. M., FULLING, K. H. & MARKS, J. E. (1985) The value of radiation therapy in addition to surgery for astrocytomas of the adult cerebrum. *Cancer*, **55**, 919–927.

GERIN, C., PALLUD, J., GRAMMATICOS, B., MANDONNET, E., DEROULERS, C., VARLET, P., CAPELLE, L., TAILLANDIER, L., BAUCHET, L., DUFFAU, H. & BADOUAL, M. (2012) Improving the time-machine: estimating date of birth of grade II gliomas. *Cell Prolif.*, **45**, 76–90.

GERLEE, P. & NELANDER, S. (2012) The impact of phenotypic switching on glioblastoma growth and invasion. *PLOS Comp. Biol.*, **8**, e1002556.

GRIER, J. T. & BATCHELOR, T. (2006) Low-grade gliomas in adults. *Oncologist*, **11**, 681–693.

GU, S., CHAKRABORTY, G., CHAMPLEY, K., ALESSIO, A. M., CLARIDGE, J., ROCKNE, R., MUZI, M., KROHN, K. A., SPENCE, A. M., ALVORD, JR, E. C., ANDERSON, A. R., KINAHAN, P. E. & SWANSON, K. R. (2012) Applying a patient-specific bio-mathematical model of glioma growth to develop virtual [18F]-FMISO-PET images. *Math. Med. Biol.*, **29**, 31–48.

HATZIKIROU, H., BASANTA, D., SIMON, M., SCHALLER, K. & DEUTSCH, A. (2012) 'Go or grow': the key to the emergence of invasion in tumour progression? *Math. Med. Biol.*, **29**, 49–65.

HIGUCHI, Y., IWADATE, Y. & YAMAURA, A. (2004) Treatment of low-grade oligodendroglial tumors without radiotherapy. *Neurology*, **63**, 2384–2386.

JAKOLA, A. S., MYRMEL, K. S., KLOSTER, R., TORP, S. H., LINDAL, S., UNSGARD, G. & SOLHEIM, O. (2012) Comparison of a strategy favoring early surgical resection vs a strategy favoring watchful waiting in low-grade gliomas. *J. Am. Med. Assoc.*, **308**, 1881–1888.

JBABDI, S., MANDONNET, E., DUFFAU, H., CAPELLE, L., SWANSON K. R., PELEGRINI-ISSAC, M., GUILLEVIN, R. & BENALI, H. (2005) Simulation of anisotropic growth of low-grade gliomas using diffusion tensor imaging. *Magn. Reson. Med.*, **54**, 616–624.

KONUKOGLU, E., CLATZ, O., BONDIAU, P. Y., DELINGETTE, H. & AYACHE, N. (2010). Extrapolating glioma invasion margin in brain magnetic resonance images: suggesting new irradiation margins. *Med. Image Anal.*, **14**, 111–125.

MARTÍNEZ-GONZÁLEZ, A., CALVO, G. F., PÉREZ-ROMASANTA, L. A. & PÉREZ-GARCÍA, V. M. (2012) Hypoxic cell waves around necrotic cores in glioblastoma: a biomathematical model and its therapeutic implications. *Bull. Math. Biol.*, **74**, 2875–2896.

MURAGAKI, Y., CHERNOV, M., MARUYAMA, T., OCHIAI, T., TAIRA, T., KUBO, O., NAKAMURA, R., ISEKI, H., HORI, T. & TAKAKURA, K. (2008) Low-grade glioma on stereotactic biopsy: how often is the diagnosis accurate? *Minim. Invasive Neurosurg.*, **51**, 275–279.

MURRAY, J. D. (2007) *Mathematical Biology: I. An Introduction*. Berlin: Springer.

OLSON, J. D., RIEDEL, E. & DEANGELIS, L. M. (2000) Long-term outcome of low-grade oligodendroglioma and mixed glioma. *Neurology*, **54**, 1442–1448.

ONISHI, M., ICHIKAWA, T., KUROZUMI, K. & DATE, I. (2011) Angiogenesis and invasion in glioma. *Brain Tumor Pathol.*, **28**, 13–24.

PAINTER, K. J. & HILLEN, T. (2013) Mathematical modelling of glioma growth: the use of Diffusion Tensor Imaging (DTI) data to predict the anisotropic pathways of cancer invasion. *J. Theoretical Biol.*, **323**, 25–39.

PALLUD, J., LLITJOS, J. F., DHERMAIN, F., VARLET, P., DEZAMIS, E., DEVAUX, B., SOUILLARD-SCEMAMA, R., SANAI N, KOZIAK, M., PAGE, P., SCHLIENGER, M., DAUMAS-DUPORT, C., MEDER, J. F., OPPENHEIM, C. & ROUX F. X. (2012b) Dynamic imaging response following radiation therapy predicts long-term outcomes for diffuse low-grade gliomas. *Neuro-Oncology*, **14**, 496–505.

PALLUD, J., TAILLANDIER, L., CAPELLE, L., FONTAINE, D., PEYRE, M., DUCRAY, F., DUFFAU, H. & MANDONNET, E. (2012a) Quantitative morphological MRI follow-up of low-grade glioma: a plead for systematic measurement of growth rates. *Neurosurgery*, **71**, 729–740.

PÉREZ-GARCÍA, V. M., CALVO, G. F., BELMONTE-BEITIA, J., DIEGO, D. & PÉREZ-ROMASANTA, L. (2011). Bright solitary waves in malignant gliomas. *Phys. Rev. E*, **84**, 021921.

PÉREZ-GARCÍA, V. M. & MARTÍNEZ-GONZÁLEZ, A. (2012) Hypoxic ghost waves accelerate the progression of high-grade gliomas. *J. Theor. Biol.* (2013).

PIGNATTI, F., VAN DEN BENT, M., CURRAN, D., DEBRUYNE, C., SYLVESTER, R., THERASSE, P., AFRA, D., CORNU, P., BOLLA, M., VECHT, C. & KARIM, A. B. (2002) Prognostic factors for survival in adult patients with cerebral low- grade glioma. *J. Clin. Oncol.*, **20**, 2076–2084.

POURATIAN, N. & SCHIFF, D. (2010) Management of low-grade glioma. *Curr. Neurol. Neurosci. Rep.*, **10**, 224–231.

ROCKNE, R., HENDRICKSON, K., LAI, A., CLOUGHESY, T., ALVORD, JR, E. C. & SWANSON, K. R. (2010). Predicting the efficacy of radiotherapy in individual glioblastoma patients in vivo: a mathematical modeling approach. *Phys. Med. Biol.*, **55**, 3271–3285.

RUIZ, J. & LESSER, G. J. (2009) Low-grade gliomas. *Curr. Treat. Opt. Oncol.*, **10**, 231–242.

SATTINGER, D. H. (1976) On the stability of waves of nonlinear parabolic systems. *Adv. Math.*, **22**, 312–355.

SMITH, J. S., CHANG, E. F., LAMBORN, K. R., CHANG, S. M., PRADOS, M. D., CHA, S., TIHAN, T., VANDENBERG, S., MCDERMOTT, M. W. & BERGER, M. S. (2008) Role of extent of resection in the long-term outcome of low-grade hemispheric gliomas. *J. Clin. Oncol.*, **26**, 1338–1345.

STAMATAKOS, G. S., ANTIPAS, V. P. & UZUNOGLU, N. K. (2006a) A spatiotemporal patient individualized simulation model of solid tumor response to chemotherapy in vivo: the paradigm of glioblastoma multiforme treated by temozolomide. *IEEE Trans. Biomed. Eng.*, **53**, 1467–1477.

STAMATAKOS, G. S., ANTIPAS, V. P. & UZUNOGLU, N. K. (2006b) Simulating chemotherapeutic schemes in the individualized treatment context: the paradigm of glioblastoma multiforme treated by temozolomide in vivo. *Comp. Biol. Med.*, **36**, 1216–1234.

SUZUKI, S. O., KITAI, R., LLENA, J., LEE, S. C., GOLDMAN, J. E. & SHAFIT-ZAGARDO, B. (2002). MAP-2e, a novel MAP-2 isoform, is expressed in gliomas and delineates tumor architecture and patterns of infiltration. *J. Neuropathol. Exp. Neurol.*, **61**, 403–412.

SWANSON, K. R., ROSTOMILY, R. C. & ALVORD, JR, E. C. (2008). A mathematical modelling tool for predicting survival of individual patients following resection of glioblastoma: a proof of principle. *Br. J. Cancer*, **98**, 113–119.

TANAKA, M. L., DEBINSKI, W. & PURI, I. K. (2009) Hybrid Mathematical model of glioma progression. *Cell. Prolif.*, **42**, 637–646.

VAN DEN BENT, M. J., AFRA, D., DE WITTE, O., BEN HASSEL, M., SCHRAUB, S., HOANG-XUAN, K., MALMSTRÖM, P. O., COLLETTE, L., PIÉRART, M., MIRIMANOFF, R. & KARIM, A. B. (2005) Long-term efficacy of early versus delayed radiotherapy for low-grade astrocytoma and oligodendroglioma in adults: the EORTC 22845 randomised trial. *Lancet*, **366**, 985–990.

VAN DER KOGEL, A. & JOINER, M. (2009) *Basic Clinical Radiobiology*. Oxford: Oxford University Press.

VOLPERT, V. & PETROVSKII, S. (2009) Reaction-diffusion waves in biology. *Phys. Life Rev.*, **6**, 267–310.

WANG, C. H., ROCKHILL, J. K., MRUGALA, M., PEACOCK, D. L., LAI, A., JUSENIUS, K., WARDLAW, J. M., CLOUGH-ESY, T., SPENCE, A. M., ROCKNE, R., ALVORD, JR E. C. & SWANSON, K. R. (2009). Prognostic significance of growth kinetics in newly diagnosed glioblastomas revealed by combining serial imaging with a novel biomathematical model. *Cancer Res.*, **69**, 9133–9140.

XIN, J. (2000) Front propagation in heterogeneous media. *SIAM Rev.*, **42**, 161–230.

Appendix. Study of the system without diffusion

A.1 *Motivation and simplified model*

The main focus of the paper is the obtention of results on LGG progression that is related to the tumour size if the transition to malignancy is not taken into account. However, it is interesting to note that a lot of information on the kinetic part of equations (2.2) can be obtained. Thus, in this appendix, we will study the pair of ordinary differential equations

$$\frac{dA}{dt} = \rho(1 - A - B)A, \tag{A.1a}$$

$$\frac{dB}{dt} = -\frac{\rho}{k}(1 - A - B)B, \tag{A.1b}$$

where now both $A(t)$ and $B(t)$ are positive functions depending only on time and describing the evolution of both tumour cell populations in systems without spatial inhomogeneities. The effect of radiotherapy given at times $(t_1, \ldots, t_n)$ with doses $(d_1, \ldots, d_n)$ and survival fractions $(S_f(d_1), \ldots, S_f(d_n))$ in this simplified model is given by the equations

$$A(t_j^+) = S_f(d_j)A(t_j^-), \tag{A.2a}$$

$$B(t_j^+) = B(t_j^-) + [1 - S_f(d_j)]A(t_j^-). \tag{A.2b}$$

A.2 *Analysis of equations* (A.1)

Since Equations (A.1) correspond to an autonomous planar dynamical system, the possible dynamics in the phase space can be completely understood. First of all, note that there are two families of equilibria. First, the equilibrium point with $(A, B) = (0, 0)$ and then the line of points $\mathcal{R}$ satisfying $A + B = 1$, with $A, B > 0$. The first one is a saddle point, thus unstable and means that tumour cells tend to regrow no matter how small is their density. With regards to those in $\mathcal{R} = \{(a, 1 - a), \ 0 < a < 1\}$, the Jacobian
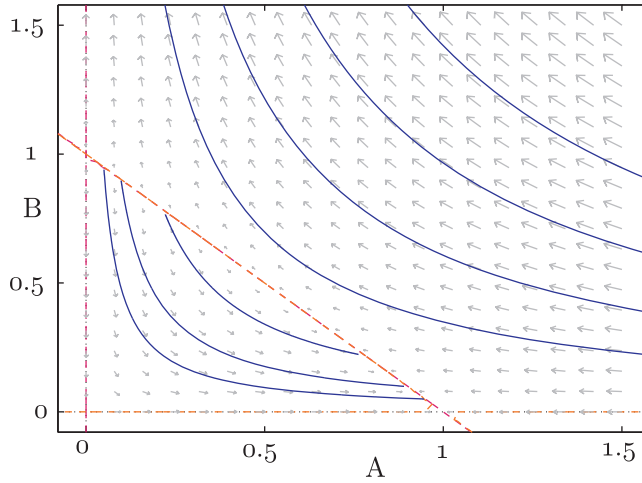
FIG. A1. Phase portrait of the dynamical system (A.1). Shown are the velocity field (arrows) and some orbits (blue) including some heteroclinic orbits connecting unstable equilibrium points on $\mathcal{R}$ with stable equilibria on the same set (blue). Also in red are shown the stable and unstable manifold of the point $(0,0)$ (located on the axes), and the manifold of equilibria $\mathcal{R}$. The red lines determine the limits of the invariant region $\mathcal{S}$.

matrix reads

$$J(\mathcal{R}) = \rho \begin{pmatrix} -a & -a \\ (1-a)/k & (1-a)/k \end{pmatrix}. \tag{A.3}$$

The eigenvalues of this Jacobian matrix are given by

$$\lambda_1 = 0, \quad \lambda_2 = \frac{\rho}{k}(1-a) - \rho a,$$

and the corresponding eigenvectors are $(1, -1)$ and $(1, -(1-a)/ka)$, respectively (for $\lambda_2 \neq 0$). The equilibrium points on $\mathcal{R}$ are non-hyperbolic points. If $a < 1/(k+1)$, then the fixed point $(a, 1-a)$ possesses a local unstable manifold and a local centre manifold. Otherwise, $(a, 1-a)$ has a local stable manifold and a local centre manifold. Thus, to get a heteroclinic orbit joining two points, say $(a_1, 1-a_1)$ and $(a_2, 1-a_2)$, with $a_2 > a_1$, it is a necessary condition that $a_2 > 1/(k+1)$ and $a_1 < 1/(k+1)$.

A straightforward application of the centre manifold theory shows that the centre manifold of $\mathcal{R}$ is the same set, i.e. $W^c(\mathcal{R}) = \mathcal{R}$. Moreover, the points of $\mathcal{R}$ satisfying $a < 1/(k+1)$ are unstable, while the points over the centre manifold satisfying $a > 1/(k+1)$ are stable.

The explicit form of the equation of the orbits can be obtained from Equations (A.1)

$$\frac{dA}{dB} = -k\frac{A}{B} \tag{A.4}$$

which leads to

$$AB^k = C, \tag{A.5}$$

with $C = A_0 B_0^k$, where $A(0) = A_0 > 0, B(0) = B_0 > 0$. Thus, the orbits correspond to hyperbolas. Some orbits together with the velocity field are shown in Fig. A1. We want to note that the centre manifold is given by the red line joining the points $(1, 0)$ and $(0, 1)$.

The feasible region of our model is the set

$$\mathcal{S} = \{(A, B) : A, B > 0, \ A + B \leqslant 1\}.$$

Since the set $\mathcal{S}$ is bounded by the centre manifold and by the line orbits of the saddle point $A = 0$ and $B = 0$, it is straightforward to see that the region $\mathcal{S}$ is an invariant region, that is, all the orbits inside $\mathcal{S}$ belong to $\mathcal{S}$ for all times $t \in \mathbb{R}$. Therefore, all the orbits inside $\mathcal{S}$ start and end in the centre manifold (except for the line orbits asymptotically approaching the saddle point $(0, 0)$ for $t = \pm\infty$).

A.3 *Exact solutions*

It is interesting to note that in special cases it is possible to compute some explicit solutions for equations (A.1). One of the most relevant cases corresponds to $k = 1$, which, as has been discussed through the paper, is the biologically most relevant situation. In that case, substituting the orbits equation, $AB = C$, in (A.1b), we obtain

$$\int \frac{\mathrm{d}B}{(B - 1/2)^2 + C - 1/4} = \rho(t - t_0). \tag{A.6}$$

It is interesting to note that, for solutions starting in the feasible region $A + B \leqslant 1$, a simple calculation shows that $0 < C < \frac{1}{4}$. Let us define $Q_+ = \sqrt{\frac{1}{4} - C} < \frac{1}{2}$. In that case, we can compute explicitly the integrals in Equation (A.6) to obtain

$$B(t) = \frac{1}{2} - Q_+ \tanh[Q_+ \rho(t - t_0)], \tag{A.7a}$$

$$A(t) = \frac{C}{1/2 - Q_+ \tanh[Q_+ \rho(t - t_0)]}. \tag{A.7b}$$

In the phase space, these solutions correspond to hyperbolas inside the region $\mathcal{S}$.

For the limit case $C = \frac{1}{4}$, Equations (A.6) can also be solved explicitly to obtain

$$B(t) = \frac{1}{2} - \frac{1}{\rho(t - t_0)}, \tag{A.8a}$$

$$A(t) = \frac{1}{2 - 4/\rho(t - t_0)}. \tag{A.8b}$$

This is a special case, since the solutions correspond to hyperbolas through the point $(\frac{1}{2}, \frac{1}{2})$, which is a point of the centre manifold and for which $\lambda_2 = 0$.

For completeness, we also present the solutions for the case $C > \frac{1}{4}$. In that case the solutions correspond to hyperbolas outside the region $\mathcal{S}$. Defining $Q_- = \sqrt{C - \frac{1}{4}}$, we obtain

$$B(t) = \frac{1}{2} + Q_- \tan[Q_- \rho(t - t_0)], \tag{A.9a}$$

$$A(t) = \frac{C}{1/2 + Q_- \tan[Q_- \rho(t - t_0)]}. \tag{A.9b}$$